Indicator Dilution Measurements of Lung Volumes and Alveolar Air Exchange During Breathing

HERBERT B. HECHTMAN, MICHAEL H. REID, BARRY C. DORN, and RICHARD D. WEISEL

From the Department of Surgery, Boston University School of Medicine, Boston, Massachusetts 02118

ABSTRACT A new triple tracer indicator dilution technique has been used to measure alveolar ventilation as well as air and tissue volumes in the lungs of experimental animals and man. The tracers indocyanine green, [^{131}I]antipyrine and xenon-133 were rapidly injected into the right atrium, while sampling was carried out from a peripheral artery.

Blood flow and tissue volumes were obtained by classical analysis of the indocyanine green and antipyrine concentration-time curves. A double exit-port, constant air flow model was used to analyze the xenon curves, because ventilatory loss led to incomplete recovery of the gas tracer in effluent blood. Uniform ventilation and perfusion were assumed. This analysis permitted calculation of alveolar ventilation ($\dot{V}A_{Xe}$) and functional residual capacity (FRC_{Xe}) during normal breathing.

In control studies, $\dot{V}A_{Xe}$ was similar to $\dot{V}A_{CO_2}$, obtained with the steady-state CO_2 method ($r = 0.87$), while in critically ill patients the xenon measurement was significantly lower, averaging 54% of $\dot{V}A_{CO_2}$. In theory, underestimates in $\dot{V}A_{Xe}$ and decrease in the ratio $\dot{V}A_{Xe}/\dot{V}A_{CO_2}$ relate to nonuniformity in regional ventilation and perfusion. The effect is greatest for the slightly soluble gas, xenon. The significant inverse correlation between $\dot{V}A_{Xe}/\dot{V}A_{CO_2}$ and the physiologic shunt is consistent with this postulate.

FRC_{Xe} was similar to the predicted FRC in animals but was 76% of the helium measured FRC in patients. FRC_{Xe} was significantly lower than the xenon measured air volumes during breath-holding when nonuniformity of ventilation was not operative. Lung tissue volumes in animals were 83% of gravimetric lung weights, while in patients the volumes were much lower than predicted. Nonhomogeneous lung function, including failure to perfuse the entire capillary bed, with resultant incomplete penetration of tracers into all segments of lung air and tissue, may explain these findings. The resultant errors can be significant in sick patients, and may themselves be used to study nonhomogeneities in the distribution of ventilation and volume.

Received for publication 18 March 1971 and in revised form 10 January 1973.

INTRODUCTION

Alveolar ventilation and the functional residual capacity (FRC)[1] are two indices of pulmonary function which have proven useful in the understanding and treating of abnormalities in respiratory gas exchange. The significance of these flows and volumes, lies both in their absolute values as well as in the uniformity of

[1] *Symbols used in this paper:* C (amount/ml), concentration; f (breaths/min), respiratory frequency; FA_g (ml gas/ml alveolar air), alveolar fraction of a gas, FRC (ml air), functional residual capacity during breathing; M (mass), amount of indicator injected; $\dot{Q}$ (ml/s), blood flow; R (dimensionless), fraction of injected tracer recovered in effluent blood; S, saturation of hemoglobin; t (s), time; $\dot{t}$ (s), transit time parameter, reduces to classic mean transit time when R = 1; $\dot{t}_{TOT}$ (s), total transit time from site of injection to site of sampling; $\Delta\dot{t}$ (s), difference in transits time parameters; T (s), time of one complete respiratory cycle; $\dot{V}A$ (ml air/s), alveolar ventilation —air flow through the control volume effective in tracer removal via the airway; VA (ml air), gas volume at end-expiration bounded by the "control surface", during breath-holding; $\bar{V}A$ (ml air), mean gas volume during breathing contained within the control surface; if $VD = 0$, $\bar{V}A = FRC_g + VT/2$; V_d (ml), volume penetrated by tracer particles which leave the lung via effluent blood—the control volume; VD (ml air), dead space—air volume contained within the lung, but outside the control surface; VT (ml air/breath), tidal volume; V_t, V_c (ml), tissue or capillary blood volume; λ_{gt}, λ_{ge} (dimensionless), gas partition coefficient between tissue or blood and air at 37°C; $\dot{Z}$ (ml/sec), diffusional clearance. *Subscripts:* Ap, iodoantipyrine, tissue tracer; c, capillary blood; g, gas tracer; G, indocyanine green; He, helium; i, input of the control surface; Kr, krypton-85; o, output of the control surface via effluent blood; r, reference tracer; t, tissue; Xe, xenon-133; 1, vascular segment from injection site to (i); 2, vascular segment from (o) to sampling site.

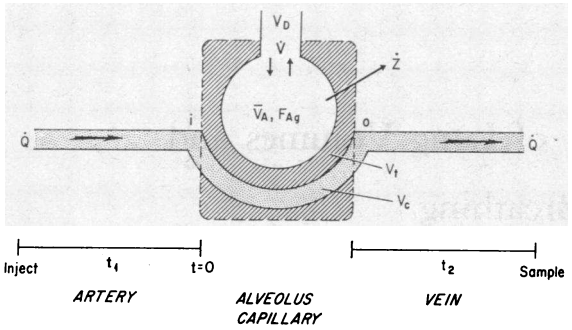

FIGURE 1 The general lung model describes a control surface (dashed line), containing the control volume. This is made up of the components: average air volume $\bar{V}_A$, tissue volume V_t, and capillary blood volume V_c. The partition coefficient of tracer gas between tissue and air is λ_{gt}, while between blood and air it is λ_{gc}. The volume of tracer distribution V_d, is a function of these solubilities and for tracer gas $V_d = \bar{V}_A + \lambda_{gt}V_t + \lambda_{gc}V_c$. Blood flow is $\dot{Q}$. The alveolar fraction of tracer gas is F_{A_g}. Tracer may leave the control volume through the airways by means of ventilation $\dot{V}_A$ or diffusion. Tracer removal by diffusion, either through the airways or pleural surface is termed diffusional clearance $\dot{Z}$, such that $\dot{Z}F_{A_g}$ is the mass of tracer cleared per second. Dead space air V_D, is beyond the control surface. Tracer injection and sampling site take place outside the control surface. The time of tracer transit from injection site to the input (i) of the control surface is t_1 while t_2 is the time of transit from the output (o) to the sampling site. At time $t = 0$, tracer crosses the input surface.

their distribution in the lungs. Thus, either absolute hypoventilation or severe non-uniformity in ventilation may result in abnormal blood gas tensions (1). Decreases in the FRC have been associated with arterial hypoxemia. A normal chest X ray under these circumstances has led to the suggestion that right-to-left shunting is taking place through areas of microatelectasis (2). The same association of hypoxemia and reduction in the FRC has been described in patients who develop stiff lungs following trauma or sepsis (3). The major cause of shunting in this situation is postulated to be an intermittant ventilation-perfusion imbalance related to alveolar collapse at end-exhalation or FRC (4). Thus, during a phase of the respiratory cycle there is perfusion of airless lung segments. This report describes a new indicator dilution method for the measurement of ventilation and air volumes in perfused regions of the lungs.

The general principles of the multiple indicator dilution technique, assumptions and equations for the calculation of flow have been discussed by Zierler and Chinard et al. (5, 6). Application to the lung, or any organ, requires injection into the inflowing stream and blood sampling from the vascular outflow. It is usually assumed that a single exit-port is present and that all tracer eventually appears in the venous effluent.

The study of the ventilated lung with gas tracers requires special consideration. Under such circumstances two exit-ports exist. Tracer gas injected as a bolus into input blood may leave the lung through either of two parallel flow channels, blood vessels and airways. In theory, the fraction of gas tracer injected which is recovered in effluent blood is defined by solubility, blood flow, ventilation, and diffusional clearance. Measurement of the recovery fraction may in turn be used to determine these flows or clearances. The mean transit time of gas tracer particles recovered in effluent blood is defined by the ratio: volume of tracer distribution/sum of the parallel flows or clearances. Measurement of the mean transit time therefore provides sufficient additional information to measure the volume of gas tracer distribution.

THEORETICAL CONSIDERATIONS

The general lung model is shown in Fig. 1. The control volume includes the perfused capillary bed which permits diffusion of blood-born tracers into the surrounding tissue V_t, and alveolar air spaces $\bar{V}_A$. Nonperfused regions (anatomic and physiologic dead space) lie outside the control volume and are excluded from this analysis. The model assumes that the ventilation/perfusion ratio is uniform throughout the lung. Time $t = 0$ occurs when the tracer crosses the control surface at point (*i*) (input) as C_i. Tracer leaves the control surface at (*o*) (output) as C_o. The tissue and air space components are limited to those regions into which tracer can both penetrate and return to capillary blood to exit via port (*o*).

In the case of the inert gas xenon, we assume that there is no diffusion limitation between alveolar gas and blood (7). Therefore the capillary blood (c) concentration at the output (o) is $C_{Xeco} = \lambda_{Xec}F_{AXe}$, where λ_{Xec} is the partition coefficient between blood and gas and F_{AXe} is the fraction of xenon in the control air volume. Blood flow is assumed to be constant since observations of tracer concentration are made over many cardiac cycles. Tissue and capillary blood volume are also considered constant.

Let us assume that tracer is rapidly injected at (i). $C(t)$ is monitored at point (o) as $C_{co}(t)$. Delays t_1 and t_2 are considered later. The mean transit time parameter is defined as

$$\dot{t} = \frac{\int_0^\infty tC_{co}(t)dt}{\int_0^\infty C_{co}(t)dt}. \quad (1)$$

When all injected tracer leaves the control volume by way of (o), the transit time parameter becomes the "classic" mean transit time and

$$\dot{t} = \frac{V_d}{\lambda\dot{Q}}. \quad (2)$$

Blood flow $\dot{Q}$ is defined as

$$\dot{Q} = \frac{M_r}{\int_0^\infty C_{rco}(t)dt}, \quad (3)$$

where M_r is milligrams indocyanine green and $C_{rco}(t)$ is the concentration of reference tracer at the output at time t. Tracer recovery must be complete.

THEORETICAL RESULTS

Breath-holding, $R_g = 1$. General indicator dilution theory is directly applicable to this single exit-port model (5). The air volume V_A, is assumed constant, therefore the respiratory quotient is 1. Tracer gas is distributed according to its solubility coefficient λ, in air, tissue, and blood. The volume equation 2 which relates the control volume to the product of blood clearance $\lambda_{gc}\dot{Q}$, and mean transit time is

$$V_A + \lambda_{gt}V_t + \lambda_{gc}V_c = \lambda_{gc}\dot{Q}\dot{t}_g. \quad (4)$$

The blood volume V_c, an element of the control volume, is defined by the reference tracer as

$$V_c = \dot{Q}\dot{t}_r, \quad (5)$$

where $\dot{t}_r$ is the transit time through lung capillaries.

The general lung model (Fig. 1) assumes that tracer injection and sampling are remote from the control surface. The absolute values of $\dot{t}_g$, $\dot{t}_{Ap}$, or $\dot{t}_r$, the mean transit times in the control volume, cannot be measured directly. This is so because the mean intravascular transit delays from injection site to (i) ($\dot{t}_1$) and from (o) to the sampling site ($\dot{t}_2$) are unknown. Therefore, $t = 0$, when tracer enters the control surface is not defined. It may be stated that the total mean transit time of the reference indicator (r) from the site of injection to the site of sampling is

$$\dot{t}_{rTOT} = \dot{t}_{r1} + \dot{t}_r + \dot{t}_{r2}. \quad (6)$$

Further, it is reasonable to assume that $\dot{t}_{g1} = \dot{t}_{r1}$ and $\dot{t}_{g2} = \dot{t}_{r2}$. It has been found that in the dog lung, the mean transit time of red cells is 0.3 s shorter than plasma (8). Knowing that xenon is two times more soluble in red cells than plasma (9), the error incurred by assuming that the transit delays 1 and 2 are the same for xenon and indocyanine green, is 0.2 s. Since the average experimental $\Delta\dot{t}_{Xe-r}$ exceeds 20 s (Tables II, III) there will be an underestimation of $\Delta\dot{t}_{Xe-r}$ of approximately 1.0% when (r) is indocyanine green.[2]

Therefore

$$\dot{t}_{gTOT} = \dot{t}_{r1} + \dot{t}_g + \dot{t}_{r2} \quad (7)$$

and

$$\dot{t}_g = \dot{t}_{gTOT} - \dot{t}_{r1} - \dot{t}_{r2}. \quad (8)$$

Equation 5 becomes:

$$V_c = \dot{Q}(\dot{t}_{rTOT} - \dot{t}_{r1} - \dot{t}_{r2}). \quad (9)$$

Equation 4 becomes:

$$V_A + \lambda_{gt}V_t + \lambda_{gc}V_c = \lambda_{gc}\dot{Q}(\dot{t}_{gTOT} - \dot{t}_{r1} - \dot{t}_{r2}). \quad (10)$$

Multiplying equation 9 by λ_{gc} and subtracting from equation 10 gives

$$V_A + \lambda_{gt}V_t = \lambda_{gc}\dot{Q}\Delta\dot{t}_{g-r}, \quad (11)$$

where we define

$$\Delta\dot{t}_{g-r} = \dot{t}_{gTOT} - \dot{t}_{rTOT}. \quad (12)$$

[2] In a strict sense, precise measure of $\Delta\dot{t}_{Xe-r}$ requires a reference tracer which is distributed in red cells and plasma exactly as xenon. An alternative is the use of both a plasma and red cell indicator (8).

Breath-holding and constant ventilation, $R_g < 1$. Under most circumstances tracer gas recovery in effluent blood is <1. The remaining tracer may diffuse or be transported by ventilation from the control volume through a second parallel flow channel, and exit the lung through a port other than (o).

Diffusion is defined as a flow or clearance, $\dot{Z}$. It is the volume of air completely cleared of tracer per second and is assumed constant. This requires that there be a steady-state flux, without back diffusion, across a fixed barrier such as the pleural surface. $\dot{Z}$ is determined by the diffusion constant and geometric parameters of the system, which include the area and thickness of the barrier. Ventilatory clearance $\dot{V}_A$, is assumed to be constant. This requires that there be continuous and uniform air flow through the control volume at a rate $\dot{V}_A$ ml/s. Since the control volume contains no dead space, all air entering this region will be effective in tracer removal. The average size of the control volume will be $\bar{V}_A$ plus the tissue and blood components.

The total mass of gas tracer leaving the control volume will be the sum of tracer mass leaving from the two exit-ports, measured over the time period required for washout. Providing tracer is not entrapped within the control volume, the mass exiting will be equal to M_0, the mass injected. For the purposes of this discussion, M_g[3] is defined by the units, milliliters of gas at 1 atm pressure and 37°C. C_{gco} is milliliters of gas dissolved in 1 ml blood at the same temperature and pressure. If at any time t, there is concentration equilibrium, then $\lambda_{gc}F_{Ag}(t) = C_{gco}(t)$. The mass flow at time t may therefore be defined for both exit ports as the product of the respective flows and concentrations: $\lambda_{gc}\dot{Q}F_{Ag}(t)$, $\dot{Z}F_{Ag}(t)$, and $\dot{V}_AF_{Ag}(t)$. Summing these mass flows over a very long period of time yields: tracer mass recovered in effluent blood, $\lambda_{gc}\dot{Q}\int_0^\infty F_{A0}(t)dt$; and that not recovered in blood, $\dot{Z}\int_0^\infty F_{Ag}(t)dt$ and $\dot{V}_A\int_0^\infty F_{Ag}(t)dt$. Therefore

$$M_g = \lambda_{gc}\dot{Q}\int_0^\infty F_{Ag}(t)dt + \dot{Z} \times \int_0^\infty F_{Ag}(t)dt + \dot{V}_A\int_0^\infty F_{Ag}(t)dt \quad (13)$$

Dividing by M_g, the fraction of injected tracer recovered in blood is

$$R_g = \lambda_{gc}\dot{Q}\int_0^\infty \frac{F_{Ag}(t)dt}{M_g}. \quad (14)$$

Substituting equation 14 into equation 13

$$\dot{V}_A + \dot{Z} = \frac{1 - R_g}{\int_0^\infty \frac{F_{Ag}(t)dt'}{M_g}}, \quad (15)$$

and since the denominator is $R_g/\lambda_{gc}\dot{Q}$

$$\dot{V}_A + \dot{Z} = \left(\frac{1}{R_g} - 1\right)\lambda_{gc}\dot{Q}. \quad (16)$$

During breath-holding when $\dot{V}_A = 0$, equation 16 may be used to define diffusional clearance. During breathing, evidence indicates that $\dot{V}_A \gg \dot{Z}$ (10). Therefore equation 16

[3] In Methods, M_g is counts per minute. C_{gco} is counts/min per milliliter of blood; F_{Ag} becomes a concentration term, counts/min per milliliter alveolar air.

reduces to

$$\dot{V}_A = \left(\frac{1}{R_g} - 1\right)\lambda_{ge}\dot{Q} \quad (17)$$

or

$$R_g = \frac{1}{1 + \frac{\dot{V}_A}{\lambda_{ge}\dot{Q}}} \quad (17a)$$

for constant ventilation.

The mean transit time for a single exit-port system is equal to the ratio: volume/flow or clearance (5). Equation 2 is applicable to the lung when an intravascular reference tracer is used. In this case the denominator of equation 2 is blood flow, $\dot{Q}$. If a gaseous tracer gains entry to the extravascular space but still exits the lung through port (o), the denominator of equation 2 is modified by λ_{ge} in order to describe the flow effective in tracer washout or clearance $\lambda_{ge}\dot{Q}$. When a second parallel flow channel washes tracer from the control volume, equation 2 will hold if the two flow channels mix at port (o). In this case the parallel flows are summed by the system. However, when the parallel flows exit through separate ports, equation 2 must be rewritten

$$i_g = \frac{V_d}{\text{flow } 1 + \text{flow } 2 \ldots .} \quad (18)$$

If there is concentration equilibrium in the control volume, such that λ_{ge} describes the tracer partition coefficient between blood and air, then the flows or clearances in the denominator of equation 18 become

$$i_g = \frac{V_d}{\lambda_{ge}\dot{Q} + \dot{V}_A + \dot{z}}. \quad (19)$$

The denominator of equation 19 will now be examined with respect to tracer recovery in effluent blood. Flow which is effective in removing the intravascular tracer from the control volume is defined by equation 3. In an analagous equation, the flows clearing tracer gas from V_d are

$$\dot{Q} + \frac{\dot{V}_A + \dot{z}}{\lambda_{ge}} = \frac{M_g}{\int_0^\infty C_{geo}(t)dt}. \quad (20)$$

Rewriting equation 14

$$R_g = \dot{Q}\int_0^\infty \frac{C_{geo}(t)dt}{M_g} \quad (14a)$$

and combining with equation 20 yields

$$\frac{\lambda_{ge}\dot{Q}}{R_g} = \lambda_{ge}\dot{Q} + \dot{V}_A + \dot{z}, \quad (21)$$

which states that blood clearance divided by the fractional recovery of tracer gas in effluent blood equals the sum of the flows or clearances acting on tracer in the control volume. V_d is defined in Fig. 1. Equation 19 becomes

$$i_g = \frac{V_A + \lambda_{gt}V_t + \lambda_{ge}V_c}{\lambda_{ge}\dot{Q}/R_g} \quad (22)$$

for breath-holding, and

$$i_g = \frac{\bar{V}_A + \lambda_{gt}V_t + \lambda_{ge}V_c}{\lambda_{ge}\dot{Q}/R_g} \quad (23)$$

for constant ventilation.

Multiplying equation 9 by λ_{ge}/R_g and subtracting from equations 22 and 23 yields equations 24 and 25.

$$V_A + \lambda_{gt}V_t + \lambda_{ge}V_c\left(1 - \frac{1}{R_g}\right) = \frac{\lambda_{ge}\dot{Q}\Delta i_{g-r}}{R_g} \quad (24)$$

$$\bar{V}_A + \lambda_{gt}V_t + \lambda_{ge}V_c\left(1 - \frac{1}{R_g}\right) = \frac{\lambda_{ge}\dot{Q}\Delta i_{g-r}}{R_g} \quad (25)$$

where Δi_{g-r} is equivalent to the difference in transit times of gas and reference tracers from the site of injection to site of sampling (equation 12). Since $\lambda_{Xec} = 0.18$ (9), R_{Xe} averages 0.23 (Table II), and V_c is approximately 4% of the air volume of the normal lung: V_A or $\bar{V}_A \gg \lambda_{ge}V_c\left(1 - \frac{1}{R_g}\right)$. Therefore, the term $\lambda_{ge}V_c\left(1 - \frac{1}{R_g}\right)$ may be eliminated from equations 24 and 25 such that

$$V_A + \lambda_{gt}V_t = \frac{\lambda_{ge}\dot{Q}\Delta i_{g-r}}{R_g}. \quad (26)$$

The average air volume $\bar{V}_A = FRC_g + V_T/2$ when $V_D = 0$. Since the tidal volume is normally distributed both to areas of dead space as well as to the control volume, $T\dot{V}_A/2$ is substituted for $V_T/2$. The equation describing constant ventilation becomes

$$FRC_g + \lambda_{gt} + \frac{T\dot{V}_A}{2} = \frac{\lambda_{ge}\dot{Q}\Delta i_{g-r}}{R_g}. \quad (27)$$

Oscillatory ventilation. The normal respiratory pattern is periodic ventilation. Classical indicator dilution theory assumes constancy of flow and constancy of the control volume (5). Oscillatory ventilation appears to violate these assumptions. Fortunately however, air flow and volume changes vary together. Under these conditions, and especially if the changes in flow and volume are rapid and phasic, the oscillatory ventilation model will reduce to constant ventilation. The maximum error in FRC_g using equation 27 will occur when respiratory cycling is extremely slow, and the entire indicator dilution curve is drawn during one respiratory phase. Thus, during the phase end-exhalation FRC_g, will equal the true FRC but during end-inhalation FRC_g will overestimate true FRC by the factor $T\dot{V}_A$. The percentage volume error will be reduced as the ratio V_T/V_d or more exactly $T\dot{V}_A/V_d$ becomes small. Under most circumstances $T\dot{V}_A$ is much less than the volume of air contained within the lung. For this reason as well as the fact that respiratory frequency is relatively rapid, our choice of the continuous flow model appears to be a reasonable approximation.

METHODS

Animals. Mongrel dogs and monkeys were anesthetized with sodium pentobarbital, intubated, and placed on their backs. Control experiments were conducted during spontaneous breathing as well as during mechanical ventilatory assistance with a piston pump.

Two dogs were bled into a reservoir and their arterial pressures maintained at 50 mm Hg. After 1 h of hypotension, indicator dilution studies were done. Another two animals were kept hypotensive for 2 h. They were studied 1 h after the reinfusion of shed blood. Autopsies were conducted at the termination of all animal experiments. The blood drained lungs were weighted, dried to constant weight and examined histologically.

TABLE I
Patient Studies

Exp.	Age	Body surface area	Diagnosis	Operation	Condition	Autopsy lung wt
		m^2				g
14	49	1.59	Hepatoma	Right hepatic lobectomy	Uneventful recovery	—
15	73	1.48	Embolus to superior mesenteric artery; 90% small bowel infarction	Embolectomy; bowel resection	Septic	1,500 10 days post-op.
16	58	1.76	Reflex esophagitis	Esophagogastrectomy	Mediastinitis, acute tubular necrosis	1,760 28 days post-op.
17	41	1.94	Coronary insufficiency; severe congestive failure	Attempted coronary bypass	Slow recovery	—
18	59	1.88	Coronary insufficiency; compensated congestive failure	Coronary bypass graft	Arrhythmia	No autopsy
19	51	1.38	Mitral stenosis and insufficiency	Mitral valve replacement	Uneventful recovery	—

Five anesthetized dogs were given succinylcholine and their ventilation controlled. Indicator studies were done in rapid sequence during breath-holding at end-expiration and during breathing. The order of this sequence, breath-holding or breathing was varied.

Three in vitro studies were conducted in the left lower lobe of a dog at 37°C, during breath-holding at end-expiration and during breathing. Recirculation was eliminated during indicator runs. Details of the perfusion apparatus have been described (11).

Patients were selected for study, either because they were suffering acute arterial hypoxemia, or because their disease or the major surgical procedure indicated for its treatment, made the patient vulnerable to pulmonary complications (Table I). Most patient studies were conducted during mechanical ventilatory assistance with an endotracheal tube in place. Control of the airway in the one patient without an endotracheal tube was accomplished with nose clips and a mouthpiece (ex. 14).

Respiratory measurements. A 7 l spirometer (Warren E. Collins, Inc., Braintree, Mass.) was used to measure tidal volume V_T, and respiratory frequency. The functional residual capacity FRC_{He}, was determined by helium dilution after switching the subject from the respirator to the Collins spirometer circuit. All patients demonstrated adequate ventilatory exchange during the several minutes required to reach helium equilibrium. Expired air was collected in small meteorologic balloons and analyzed for CO_2 tension with the Severinghaus electrode.

Hemodynamic measurements. All subjects had right atrial and either carotid or brachial arterial catheters. The brachial artery was utilized in patients. In addition, all patients had a balloon-tipped catheter (Swan-Garz, Edwards Laboratory, Santa Ana, Calif.) positioned in a distal pulmonary artery. On occasion this catheter was coupled to a strain gauge transducer to give pulmonary arterial and wedge pressures.

Physiologic shunt $\dot{Q}_S/\dot{Q}$. The partial pressures of oxygen and carbon dioxide were measured with Clark and Severinghaus electrodes (IL 213, Instrumentation Laboratories, Lexington, Mass.), in blood drawn from arterial and right atrial (animals), or pulmonary arterial (patients) catheters. Arterial C_a and mixed venous $C_{\bar{v}}$ oxygen contents were then calculated from the hemoglobin concentration measured by oximetry and the derived value for hemoglobin saturation. The latter was obtained from standard nomograms describing the oxygen hemoglobin dissociation curve. The alveolar gas equation was used to calculate end-capillary oxygen content C_c. The fraction of blood flow passing through the lungs, having the same oxygen content as mixed venous blood, was obtained from the formula

$$\frac{\dot{Q}_S}{\dot{Q}} = \frac{C_{cO_2} - C_{aO_2}}{C_{cO_2} - C\bar{v}_{O_2}}. \quad (28)$$

Indicator dilution studies. The three tracers employed were: indocyanine green as the intravascular marker; iodoantipyrine ([^{131}I]antipyrine, 20 μCi, Amersham/Searle Corp., Arlington Heights, Ill.) for the extravascular tissue space; and a saline solution of xenon-133 (200 μCi, New England Nuclear Corp., Boston, Mass.) for both the extravascular tissue and air spaces. An isosmotic tracer mixture was prepared anerobically and a portion saved for analysis (12). The mass of tracer injected was expressed as milligrams indocyanine green and counts per minute of ^{131}I and ^{133}Xe. Patients were pretreated with 200 mg sodium iodide to block ^{131}I uptake by the thyroid. A rapid injection of 1–2 ml of tracer mix was made into the right atrial catheter, followed by a 5 ml flush of blood. Arterial sampling was started at the moment of injection, at a rate of 23 ml/min. In small monkeys, the rate was reduced to 11.6 ml/min. Mercury spacers were used to separate samples at 1–2-s intervals (12). The concentration of indocyanine green (milligrams per milliliter) was measured spectrophotometri-

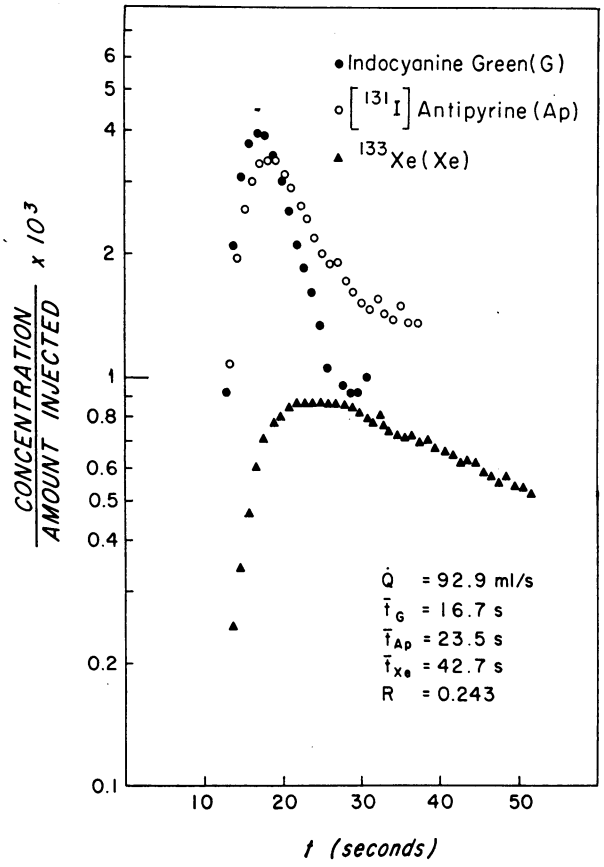

FIGURE 2 A typical triple tracer, indicator dilution run is illustrated (exp. 16*d*, Table II). The down slopes of the dye and antipyrine curves are monoexponential until the appearance of recirculation. In the case of xenon, recirculation is not seen and the downslope is monoexponential throughout. All curves have been normalized by plotting the ordinate as tracer concentration/amount injected. It is assumed that all indocyanine green leaves the lung by way of effluent blood and therefore its recovery is 1.0. Flow $\dot{Q}$, is calculated from this curve. Ventilation provides a second exit-port for xenon and results in the failure of complete recovery R, in effluent blood. R is calculated from the ratio of the areas described under the normalized xenon and indocyanine green curves. Alveolar ventilation is derived from equation 17, using $\dot{Q}$, R, and λ, the solubility coefficient of xenon. Measurement of tissue and air volumes require knowledge of the mean transit time parameters for the three tracers. These are used to calculate $\Delta\bar{t}_{Ap-G}$ and $\Delta\bar{t}_{Xe-G}$, which are the differences in mean transit times that yield tissue and air volumes by means of equations 29 and 27. Although catheter delays have been subtracted from the illustrated curves, this is not necessary to obtain $\Delta\bar{t}$.

cally, (Gilson Medical Electronics, Inc., Middleton, Wis.) while isotope concentrations (counts/minute per milliliter) were measured with a dual channel, well scintillation system (Picker Corp., Newton Upper Fall, Mass.). Since the mass of isotope injected and the concentration in effluent blood were expressed in terms of gamma energies, the fraction of ^{133}Xe in alveolar gas F_{AXe}, now becomes: counts/minute per milliliter alveolar gas at 1 atm pressure and 37°C.

Calculations. A typical set of indicator dilution curves is illustrated for experiment 16*d* (Fig. 2). All tracer downslopes were monoexponential and were extrapolated by the method of least squares to ordinate values which were 1% of peak height. The integrals $\int_0^\infty C_{co}(t)dt$ and $\int_0^\infty tC_{co}(t)dt$ were calculated according to the method of Chinard et al. (6). The mean transit time parameters $\bar{t}_G$, $\bar{t}_{Ap}$, and $\bar{t}_{Xe}$ were derived from equation 1 while blood flow $\dot{Q}$ was derived from equation 3.

Tissue volume V_t is:

$$V_t = \dot{Q}\Delta\bar{t}_{Ap-G}, \tag{29}$$

where $\Delta\bar{t}_{Ap-G}$ is the difference in mean transit times between antipyrine and indocyanine green. The partition coefficient for iodoantipyrine between tissue and blood is assumed to be 1.0.[4]

Alveolar ventilation. $\dot{V}_{AXe}$ (milliliter per second) was calculated from the xenon and indocyanine green data using the continuous air flow model of the lung (equation 17). The partition coefficient λ_{Xeb} was modified for changes in hematocrit (Hct) (13), which was measured by the capillary tube technique. The fractional recovery of injected xenon in effluent blood R_{Xe} was calculated from the normalized indicator curves by means of

$$R_{Xe} = \frac{\text{area}_{Xe}}{\text{area}_G}, \tag{30}$$

where "area" is that described under the normalized concentration time curves of xenon (Xe) and indocyanine green (G).

Alveolar ventilation (milliliter) was also derived from measurements of tidal volume V_T, mixed expired carbon dioxide tension P_{ECO_2} and arterial carbon dioxide tension P_{aCO_2}.

$$\dot{V}_{ACO_2} = \frac{V_T}{T}\left(\frac{P_{ECO_2}}{P_{aCO_2}}\right). \tag{31}$$

End-expiratory air volume. FRC_{Xe} (milliliters) during breathing was calculated from the constant airflow model (equation 27). The solubility coefficient of xenon between tissue and air $\lambda_{gt} \simeq 0.1$ (9).

RESULTS

Alveolar ventilation was measured in all subjects: 2 rhesus monkeys, 11 mongrel dogs and 6 patients (Table II). $\dot{V}_{AXe}$ was calculated from equation 17 and $\dot{V}_{ACO_2}$ from equation 31. A comparison of these measurements is given in Fig. 3. The six closed circles refer to dogs who had been subjected to hemorrhage while the 11 closed triangles refer to patients who were critically ill at the time of the study (Table I, exps. 15–18). The remaining 28 runs in control animals, and patients who made uneventful recoveries are described by the regression equation $T\dot{V}_{AXe} = (0.87)\ T\dot{V}_{ACO_2} + 12.8$ ($r = 0.87$). Alveolar ventilation calculated from xenon was 93.8% of that calculated from CO_2. During and after hemorrhagic hypotension the percentage was 77.4% ($n = 6$).[5] In the seriously ill patients $\dot{V}_{AXe}$ was

[4] Since the partition coefficient is assumed, V_t is strictly defined as an [^{131}I] antipyrine volume of distribution.

[5] n refers to the number of runs.

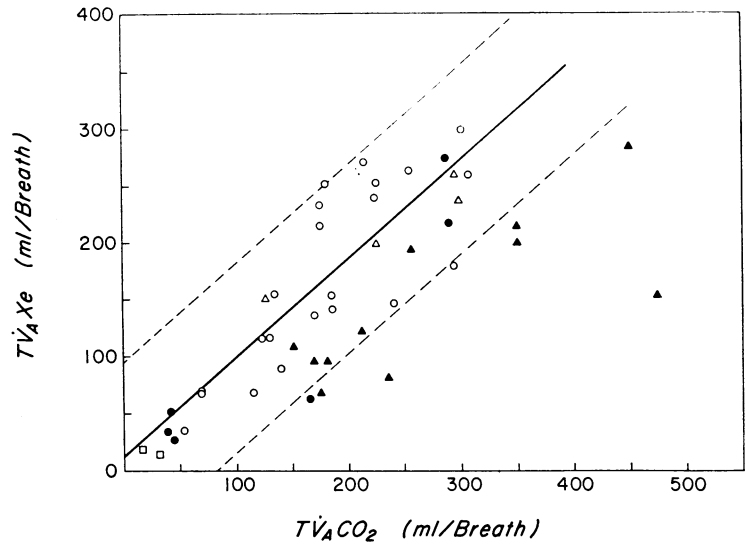

FIGURE 3 Alveolar air exchange per breath, measured by the xenon $T\dot{V}_{AXe}$, and carbon dioxide $T\dot{V}_{ACO_2}$ methods is compared. The respiratory frequency varied from 11 to 86 cycles/min. The open squares, circles, and triangles represent control monkeys, dogs, and those patients who made uneventful recoveries. This data is described by the regression equation $T\dot{V}_{AXe} = 0.87T\dot{V}_{ACO_2} + 12.8$ ($r = 0.87$). The dotted lines encompass ± 1 standard deviation. The closed circles and triangles are animals subjected to hemorrhage and patients who were critically ill.

significantly lower than $\dot{V}_{ACO_2}$ averaging 53.9% of $\dot{V}_{ACO_2}$ ($P < 0.01$).

The pulmonary tissue volume V_t in dogs, measured with the antipyrine tracer using equation 29, averaged 8.86 ml/kg$\pm$3.10 SD in 22 control runs (Table II). This was significantly lower than weights of the blood drained lungs, which averaged 10.7 ml/kg ($P < 0.05$). During hemorrhagic hypotension, the average of three runs was 5.70 ml/kg, while after the reinfusion of shed blood, the average was 12.9 ml/kg ($n = 3$). The results in these three groups demonstrate a wide scatter from the mean. The fractional recovery of antipyrine was 0.986$\pm$0.088 SD for all 28 runs.[6]

The patients also showed wide variations in the measured tissue volume. The four patients (exps. 15–18) who were seriously ill averaged 7.52 ml/kg$\pm$2.51 SD, or 274 ml/m^2 ($n = 11$), while the two patients who made uneventful recoveries (exps. 14, 19), averaged 4.70 ml/kg or 144 ml/m^2 ($n = 2$). The fractional antipyrine recovery was 0.886$\pm$0.158 SD for all patient runs ($n = 13$).

Air volumes. FRC_{Xe}, measured by the tracer technique using equation 27, averaged 34.8 ml/kg $\pm$14.5 SD in the control dogs ($n = 22$), 23.3 ml/kg in the two hypotensive animals ($n = 3$), and 15.3 ml/kg in the two animals who had their shed blood reinfused ($n = 3$) (Table II).

A tissue tracer was not used in the two monkey experiments nor in the first two patient runs (exp. 14*a*, *b*). In these runs the volume calculated from equation 27 is $FRC_{Xe} + \lambda_{gt}V_t$. The overestimate in FRC_{Xe}[7] by assuming $FRC_{Xe} \gg \lambda_{gt}V_t$ is between 3 and 4%, since the ratio $FRC_{Xe}/\lambda_{gt}V_t = 39.3$ for the 22 control runs and 28.2 for all patient runs other than 14*a* and *b*. If the assumption $FRC_{Xe} \gg \lambda_{gt}V_t$ is permitted, than FRC_{Xe} averaged 27.8 ml/kg for the two monkey runs. The two patients who made uneventful recoveries had an average FRC_{Xe} of 35.6 ml/kg ($n = 4$). In the four critically ill patients where the assumption was not necessary, FRC_{Xe} was 18.2 ml/kg ($n = 11$). The FRC_{He} was 63.3 ml/kg and 24.7 ml/kg, respectively, in these two patient groups. The FRC_{He} in exp. 17*b* is not included in these results. A prolonged delay occurred in this run, in switching the patient from the respirator to the Collins spirometer.

Five dogs were made to breath-hold at the end of a normal tidal volume (Table III). The average air volume V_{AXe} was 32.9 ml/kg (equation 26). Breathing FRC_{Xe}, and breath-holding volumes V_{AXe} were compared in sequential funs in four dogs and in three pump perfused lobes. FRC_{Xe} was lower than V_{AXe} ($P < 0.05$), averaging 87.6% of V_{AXe}. In comparing FRC_{Xe} and V_{AXe} the small error due to the tissue factor $\lambda_{gt}V_t$, tends to cancel out.

[6] $R_{Ap} = \frac{\text{area}_{Ap}}{\text{area}_G}$, *cf.* equation 30.

[7] FRC_{Xe} and V_{AXe} include air volume and the tissue factor, $\lambda_{gt}V_t$.

TABLE II
Lung Volumes and

Exp.	Weight	Hct	f*	V_T	$\dot{Q}$	$\bar{\imath}_G$	$\bar{\imath}_{Ap}$	$\bar{\imath}_{Xe}$	R_{Xe}	$\dot{Q}_S/\dot{Q}$
	kg		*cycles·min⁻¹*	*ml/breath*	*ml·s⁻¹*					
Monkeys										
1	4.9	31	18	42.8	20.0	4.6		19.7	0.370	0
2	2.7	34	18	60.5	9.6	2.5		17.3	0.277	0
Dogs‖										
3	21.5	45	18	300	24.4	11.4	18.3	46.7	0.100	0.12
4 *a*	21.0	48	13*	302	34.2	12.6	18.1	33.0	0.114	0.11
b		48	13*	302	33.6	11.7	17.5	33.8	0.105	0.08
5 *a*	21.3	51	14*	335	27.2	11.8	17.6	24.3	0.077	0.12
b		51	14*	358	31.2	10.0	16.1	25.5	0.093	0.13
6 *a*	25.4	51	18*	394	96.5	4.5	7.0	18.8	0.305	0.24
b		51	19*	394	90.0	1.7	4.5	14.3	0.263	0.21
c		45	12*	577	64.0	7.2	11.9	20.3	0.166	0.14
d		44	11*	480	70.9	6.5	10.7	23.2	0.216	0.09
7 *a*	22.2	48	25	205	47.8	11.5	15.5	45.8	0.237	0.09
b		48	32	205	55.8	9.5	14.9	30.7	0.220	0.08
c		55	20	262	46.8	12.3	17.6	33.7	0.194	0.07
d		55	22	283	43.7	12.1	16.7	30.6	0.170	0.10
8 *a*	21.9	40	14*	253	47.8	10.3	14.3	27.0	0.191	0.09
b		40	13.5*	253	43.0	11.7	18.9	26.8	0.137	0.11
9 *a*	26	42	32	243	44.6	9.0	9.8	21.1	0.181	0.25
b		42	86	131	49.9	9.7	11.1	18.6	0.153	0.17
10 *a*	19	45	14*	345	32.7	15.7	21.1	24.3	0.098	0.13
b		45	15*	350	31.7	17.5	20.2	22.1	0.082	0.15
c		45	16*	389	16.0	21.5	26.2	31.9	0.039	0.13
d		45	16*	390	13.0	20.7	25.9	30.9	0.040	0.17
11	13.5	37	25	500	9.7	27.1	40.5	34.1	0.072	0.11
12 *a*	25.8	44	19	346	72.9	5.5	9.2	29.8	0.324	0.16
b		44	23	311	71.1	5.1	8.9	22.5	0.351	0.14
13 *a*	25.8	44	14.5*	434	66.1	9.2	13.1	22.6	0.256	0.24
b		44	13*	468	62.5	10.3	12.8	22.9	0.229	0.26
c		52	50	151	29.1	13.6	23.9	22.6	0.166	0.20
d		53	68	176	24.8	15.0	32.3	26.0	0.138	0.18
Patients										
14 *a*	49	33	20	763	134	15.6		36.2	0.223	0.23
b		30	20	349	101	17.0		43.6	0.200	0.19
c		32	26	363	68.0	12.8	17.6	36.4	0.149	0.16
15 *a*	45.9	26	24*	403	47.0	27.1	33.3	49.2	0.160	0.27§
b		20	36*	372	87.7	18.8	23.6	33.9	0.167	0.29§
16 *a*	64	21	20*	469	28.8	19.1	26.0	39.3	0.159	0.21§
b		25	18*	634	47.8	17.7	24.9	33.5	0.169	0.23§
c		26	20*	564	74.6	16.6	23.8	36.0	0.153	0.17§
d		32	19*	759	92.9	16.7	23.5	42.7	0.243	0.28§
17 *a*	75	33	13*	651	77.8	23.9	33.7	51.9	0.219	0.19§
b		33	14*	881	66.7	28.7	39.9	47.6	0.145	0.15§
c		30	16*	802	80.6	27.6	36.3	57.5	0.273	0.13§
d		30	20*	401	88.3	21.9	27.8	51.4	0.267	0.19§
18	73.5	34	11*	687	61.7	23.4	28.2	55.2	0.204	0.19§
19	42.3	33	11	452	29.8	40.9	44.8	63.7	0.095	0.02

* Volume cycled respirator.
‡ Prolonged time to switch into spirometer circuit; result suspiciously low.
§ $F_{I_{O_2}}$ = 50%; unmarked signifies room air.
‖ Bracketed runs were done within 30 min of each other.

$\dot{V}_{AXe}$	$\dot{V}_{ACO_2}$	V_t	FRC_{Xe}	FRC_{He}	FRC_{Xe}/V_t	Condition		
$ml \cdot s^{-1}$	$ml \cdot s^{-1}$	*ml*	*ml*	*ml*				
5.62	4.86		127			Control		
4.30	9.57		80			Control		
40.8	51.0	168	1,517		9.03	Control		
50.8	37.9	188	1,027		5.46	Control		
54.7	39.0	195	1,198		6.14	Control		
63.3	49.9	158	705		4.46	Control		
59.0	52.5	190	863		4.54	Control		
42.7	55.8	241	782		3.25	Control		
48.9	58.6	252	734		2.91	Control		
59.8	60.2	301	760		2.52	Control		
47.6	56.3	298	854		2.87	Control		
29.4	28.6	191	1,260		6.60	Control		
37.8	36.8	301	956		3.18	Control		
38.9	41.0	248	949		3.83	Control		
42.7	47.7	201	873		4.34	Control		
36.2	31.3	191	651		3.41	Control		
48.5	39.4	310	716		2.31	Control		
36.5	61.3	36	502	2,253	13.94	Control		
50.0	76.6	69	501	1,073	7.26	Control		
56.0	52.1	177	396		2.24	Control		
66.0	63.5	85.6	190		2.22	Control		
73.1	76.3	75.0	649		8.65	Hemorrhage 50 mm Hg		
58.0	77.1	67.0	501		7.48	Hemorrhage 50 mm Hg		
21.8	17.6	130	125		0.96	Hemorrhage 50 mm Hg		
28.1	44.3	270	940		3.48	Control		
24.3	63.2	270	593		2.20	After hemorrhage		
35.5	58.2	258	541		2.10	Control		
38.9	63.7	156	531		3.40	Control		
28.7	31.7	300	262		0.87	After hemorrhage		
30.5	49.8	429	333		0.78	After hemorrhage		
						Pressure (*mm Hg*)		
						P_a	P_a wedge	Post-op., day, h
78.9	99.2		1,961	2,889		15	10	pre-op.
66.3	74.7		2,104	2,569		23	5	2
64.9	55.0	326	1,691	1,928	5.19	20	5	3
38.8	67.8	291	942	2,191	3.24	22	7	2
65.2	91.0	421	1,085	1,783	2.58	18	10	4
22.8	58.6	199	495	1,678	2.49	15	7	14
36.7	63.5	344	602	1,153	1.75	16	7.5	15, a.m.
64.8	85.3	537	1,334	1,516	2.48	17	8	15, p.m. after dialysis
48.3	150	632	1,511	1,382	2.39	18	10	20
46.9	75.6	762	1,487	1,505	1.95	30	22	0, 5 h
66.1	105	747	1,244	874‡	1.67	31	23	0, 7 h
35.2	102	701	1,337	1,396	1.91	25	19	1, a.m.
39.8	75.3	521	1,500	2,028	2.88	25	22	1, p.m.
40.9	64.2	296	1,505	1,095	5.08	30	15	0, 7 h
47.7	53.9	116	1,060	2,390	9.14			0, 7 h

TABLE III

Air Volumes during Breath Holding and Breathing

Exp.	State	f	Lung wt	$\dot{Q}$	Hct	$\Delta\bar{t}_{Xe-G}$	R_{Xe}	$\dot{Q}_S/\dot{Q}$	$\bar{V}_{AXe}$* or FRC_{Xe}	ml air‡/g lung
		cycles $\cdot min^{-1}$	*g*	$ml \cdot s^{-1}$		*s*			*ml*	
A. Pump perfused lungs										
20*a*	Breath hold	0	50	6.32	27	85.3	0.431		199	3.98
b	Breathing	14	50	5.27	27	31.4	0.134	0.13	185	3.70
c	Breathing	14	50	3.00	28	68.6	0.253	0.26	128	2.56
d	Breath hold	0	50	3.23	28	172	0.774		116	2.32
e	Breathing	14	50	3.06	28	67.0	0.264	0.26	123	2.46
21*a*	Breath hold	0	62	3.65	30	171	0.942		109	1.76
b	Breathing	15	62	3.00	30	47.6	0.244	0.16	92.9	1.50
22*a*§	Breath hold	0	75	3.54	32	46.8	1.01		27.4	0.37
b	Breathing	20	75	3.25	32	23.2	0.474	0.36	26.0	0.35
			Body wt *kg*							ml air/kg
B. Intact dogs										
23*a*	Breath hold	0	23	50.4	30	50.2	0.658		631	27.4
b	Breath hold	0	23	69.4	29	25.2	0.517		551	24.0
c	Breath hold	0	23	87.3	30	11.4	0.235		695	30.2
24*a*	Breath hold	0	32.5	99.2	35	12.0	0.175		1163	35.8
b	Breathing	14	32.5	109	35	11.0	0.173	0.24	994	30.6
25*a*	Breath hold	0	30.8	38.4	40	8.3	0.134		426	13.8
b	Breathing	14	30.8	44.3	40	8.2	0.124	0.31	404	13.1
26*a*	Breath hold	0	34.5	114	39	17.4	0.229		1542	44.7
b	Breathing	14	34.5	63.9	39	19.6	0.145	0.29	1394	40.4
27*a*	Breath hold	0	24.5	59.2	40	80.0	0.805		1053	43.0
b	Breathing	14	24.5	65.0	43	10.1	0.188	0.19	529	21.6

* $\bar{V}_{AXe}$ or $FRC_{Xe} + \lambda_{gt}V_t$.

‡ To convert ml air/g lung to ml air/kg body wt, multiply by 10.7 g lung/kg body wt.

§ Large areas of atelectasis.

DISCUSSION

Alveolar ventilation measured by the xenon method correlated well with $\dot{V}_{ACO_2}$ ($r = 0.87$) in control animals and patients who made uneventful recoveries. $\dot{V}_{AXe}$ tended to be slightly but not significantly lower than $\dot{V}_{ACO_2}$ in this group. The average was 93.8%. A highly significant difference in the measured alveolar ventilations occurred in the critically ill patients where $\dot{V}_{AXe}$ averaged 53.9% of $\dot{V}_{ACO_2}$. The two factors that may account for this discrepancy are diffusion and nonuniform ventilation-perfusion ratios.

In normal lungs, where there is minimal or no diffusion limitation across the pulmonary membrane, it is probable that tracer gases, including CO_2, diffuse beyond alveoli and enter the distal conducting airways (14). Air exchange in these distal airways effectively removes tracer, and therefore, is included in the measured "alveolar ventilation". The rate of gas diffusion will determine the depth of tracer penetration into the conducting airways. As the rate of diffusion increases, there will be an apparent decrease in wasted, dead space ventilation and an increase in $\dot{V}_A$. Carbon dioxide is lighter than xenon-133 and therefore diffuses more rapidly in air.[8] These considerations are consistent with the findings that $\dot{V}_{AXe} < \dot{V}_{ACO_2}$. Similar results have been reported using steady state techniques for the calculation of $\dot{V}_{AXe}$ and $\dot{V}_{ACO_2}$ (10). Although the findings are consistent with diffusion effects, it has been observed experimentally that during the period of a normal respiratory cycle, there is insufficient time for the diffusion separation of the gases krypton-85 and CO_2 (10).

Another possible mechanism that may produce this disparity in $\dot{V}_A$, relates to regional variations in the ventilation-perfusion ratio. The ventilation equation

[8] Graham's law states that the rate of diffusion is proportional to $\frac{1}{\sqrt{\text{density}}}$.

17 assumes a single compartment lung with a uniform $\dot{V}_A/\dot{Q}$ ratio. Under such circumstances $\dot{V}_{AXe}$ will be identical to $\dot{V}_{ACO_2}$. As the distribution of ventilation-perfusion ratios around the average ratio becomes wider, tracer recovery in effluent blood will, in theory increase. This leads to a calculated $\dot{V}_A$ which is lower than the single compartment lung (10). A theoretical example of a two compartment lung is given in Fig. 4.

Despite inhomogeneities, as long as the gas tracers have equal blood solubilities, there should be no disparity in their measured $\dot{V}_A$'s; although they will be lower than those measured in the homogeneous lung. The critical issue involves the use of tracers of different solubilities in a lung with nonuniform ventilation perfusion ratios. In theory, this will lead to discrepancies in the calculated alveolar ventilation (15). The lower the solubility, the lower the calculated $\dot{V}_A$. The experimental observation that $\dot{V}_{AXe} < \dot{V}_{ACO_2}$ is in keeping with the fact that CO_2 is much more soluble in blood than xenon. The theoretical calculations illustrated in Fig. 4 shows that a 20% anatomic shunt will lead to reductions in $\dot{V}_{AXe}$ to 42% of true ventilation while $\dot{V}_{ACO_2}$ is minimally reduced to 97.3%. The striking reduction in $\dot{V}_{AXe}$ relates to the low solubility of xenon. Only 15% of xenon entering the lung via input blood is recovered in the venous effluent. A 20% anatomic shunt results in 30% recovery. In the case of the highly soluble gas CO_2, 90.00% is normally recovered, ($\dot{V}_A/\dot{Q} = 1$, $\lambda = 9$) whereas a 20% shunt leads to a minimal increase in recovery to 90.24%. Thus, although the absolute mass of xenon cleared by ventilation may be far greater than CO_2, the reduction in the efficiency of this ventilatory clearance is much more marked for xenon in the presence of shunting. The reduced efficiency of gas exchange due to $\dot{V}_A/\dot{Q}$ inhomogeneities may be described by the ratio $\dot{V}_{AXe}/\dot{V}_{ACO_2}$.

Nonuniformity in perfusion also results in $\dot{V}_A/\dot{Q}$ imbalance and again leads to greater underestimates in $\dot{V}_{AXe}$ than $\dot{V}_{ACO_2}$ (Fig. 5). When regional perfusion is completely interrupted, that region is no longer included within the control volume. Ventilation to the region (dead space ventilation) is then unmeasured regardless of the tracer used.

These theoretical considerations demonstrate that although $\dot{V}_A$ is unchanged, the effective ventilation depends on both gas solubility and the degree of nonhomogeneity in the $\dot{V}_A/\dot{Q}$ ratios. Experimental evidence supports this postulate. A significant correlation exists between $\dot{V}_{AXe}/\dot{V}_{ACO_2}$ and $\dot{Q}_S/\dot{Q}$ measured during room air breathing ($r = -0.54$, $P < 0.001$). If the calculated shunt $\dot{Q}_S/\dot{Q}$, represents anatomic shunting (flow through nonventilated lung regions), then the experimental ratio $\dot{V}_{AXe}/\dot{V}_{ACO_2}$ should be the same as the ratio predicted from the two-compartment lung model when $\dot{V}_{A1} = 0$ (anatomic shunt). It may be seen however, that the data points fall to the right of the theoretical curve (Fig. 6). Agreement is somewhat better when $\dot{Q}_S/\dot{Q}$ is calculated during 50% oxygen breathing. These observations are in accord with the fact that $\dot{Q}_S/\dot{Q}$ becomes a better index of anatomic shunting when high concentrations of oxygen are inspired.

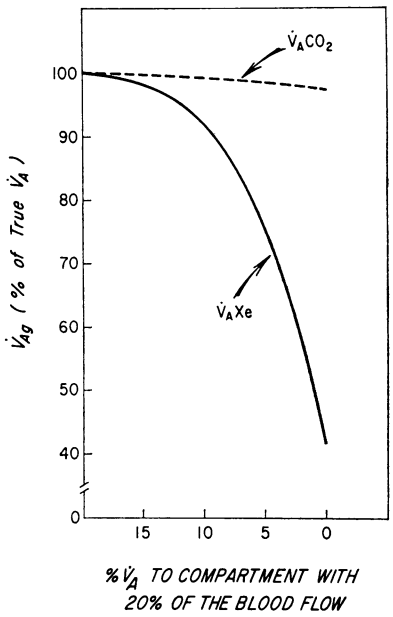

FIGURE 4 Alveolar ventilation measured with $\dot{V}_{AXe}$ underestimates true ventilation when there are ventilation-perfusion inhomogeneities. This is shown in a two-compartment lung model where compartment 1 receives 20% of blood flow $\dot{Q}_1$, and from 20% to 0% of the ventilation $\dot{V}_{A1}$. Total flow $\dot{Q}$, and ventilation $\dot{V}_A$ are constant. Tracer recovery R_g, is the sum of the recovery fractions from each compartment, weighted by flow to that compartment, and is calculated from a modification of equation 17*a*:

$$R_g = \frac{1}{\dot{V}_{A1}/\lambda\dot{Q}_1 + 1}\frac{\dot{Q}_1}{\dot{Q}} + \frac{1}{\dot{V}_{A2}/\lambda\dot{Q}_2 + 1}\frac{\dot{Q}_2}{\dot{Q}}$$

$\dot{V}_A$ gas is then calculated by substituting R_g into equation 17. Xenon is a poorly soluble gas and R_{Xe} is normally about 0.15. As $\dot{V}_{A1}$ and therefore $\dot{V}_{A1}/\dot{Q}_1$ decrease to zero, R_{Xe} will increase substantially. Since $\dot{V}_A$, $\dot{Q}$, and λ are constant $\dot{V}_{AXe}$ will decrease dramatically (solid line). The greatest rate of increase in R_{Xe} (and therefore decrease in $\dot{V}_{AXe}$) will be when the $\dot{V}_A/\dot{Q}$ ratios deviate about a mean $\dot{V}_A/\dot{Q} = \lambda_{Xe} = 0.181$ (9). In the case of the very soluble gas CO_2 where $\lambda \sim 9$ (10), recovery is usually very high (~ 0.90). Therefore $\dot{V}_{ACO_2}$ is relatively unaffected by low $\dot{V}_A/\dot{Q}$ ratios. The minimal fall in $\dot{V}_{ACO_2}$ leads to use of the ratio $\dot{V}_{AXe}/\dot{V}_{ACO_2}$ as an index of nonuniformities in regional $\dot{V}_A/\dot{Q}$.

The shunt fraction $\dot{Q}_S/\dot{Q}$, calculated from equation 28 is conceptually the same as the recovery fraction R_{Xe} (16, 17). Oxygen contents however, are primarily determined by a chemical union with hemoglobin and not by λ_{O_2}. This explains the fact that disparities exist between R_{Xe} and $\dot{Q}_S/\dot{Q}$ (Table II) and make it unlikely

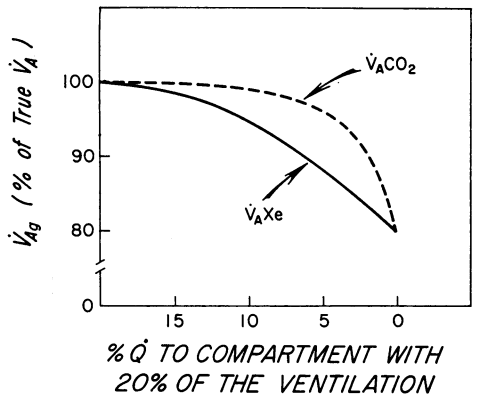

FIGURE 5 The two-compartment lung described in Fig. 4 is used to illustrate the effect of decreasing blood flow to compartment 1 from 20% to 0%, while $\dot{V}_{A_1}$ remains at 20%. Total flow and ventilation are constant. $\dot{V}_{AXe}$ and $\dot{V}_{ACO_2}$ are calculated by the method described in Fig. 4. As $\dot{Q}_1$ decreases, tracer measured $\dot{V}_{A_g}$ underestimates true ventilation. The error is greatest with xenon, the least soluble gas. When $\dot{Q}_1 = 0$, the air spaces (physiologic dead space) are no longer within the control volume and $\dot{V}_{A_1}$ is unmeasurable. In this example $\dot{V}_{ACO_2}$ is reduced to a greater extent than when inhomogenities are due to very low $\dot{V}_A/\dot{Q}$ ratios. In theory, the most pronounced changes in $\dot{V}_{ACO_2}$ will occur when the $\dot{V}_A/\dot{Q}$ ratios vary about λ_{CO_2}. As $\dot{Q}_1$ is reduced $\dot{V}_{A_1}/\dot{Q}_1$ becomes very high and equals or exceeds λ_{CO_2}.

that xenon can provide an accurate reflection of the efficiency of oxygen exchange.

Pulmonary tissue volume. In control dogs the lung tissue volume, V_t was 8.86 ml/kg. The tritiated water volume in dogs, reported in three series, averaged 3.81 ml/kg (18–20). After a correction factor was applied to account for water volume in blood, Goresky found that he was able to measure between 50–61% of the lung weight (8). V_t was 82.8% of the weight of the blood-drained lung.

The differences in the water and antipyrine measured volumes, might be due to the fact that antipyrine has access to a larger extravascular lung volume than tritiated water. The moderate fat solubility of antipyrine argues for its distribution into a larger extravascular space. If the density of the lung is one, V_t then should approach the weight of the blood drained lung.

Comparison of the volumes accessible, and those actually measured, results in better agreement. Antipyrine measures 82.8% of the lung weight while tritiated water measures 64–78% of lung water (28). The failure to measure 100% of the respective volumes is probably due to incomplete perfusion of the pulmonary capillary bed (21).

The data in patients is also consistent with this perfusion hypothesis. In the two patients who made uneventful recoveries, V_t was found to be 144 ml/m^2, while in five comparable individuals, the tritiated water space after correction for water in blood was 112 ml/m^2 (20). The predicted normal parenchymal volume is 259 ml/m^2 (22). The group of patients who were critically ill had an enlarged V_t of 274 ml/m^2. Without knowledge of the size of the perfusion bed, a precise estimate of lung weight cannot be given.

Air volumes. In control dogs, FRC_{Xe} was found to be 34.8 ml/kg while the predicted FRC is 33.1 ml/kg (23, 24). In the complete patient series, FRC_{Xe} was significantly lower than the helium measured FRC, averaging 76.5% ($P < 0.05$). Several factors may be responsible for this discrepancy in FRC_{Xe} and FRC_{He}. These are: (*1*) regional variations in the $\dot{V}_A/\dot{Q}$ ratio, (*2*) restriction in the volume available to xenon because of (*a*) diffusion limitations and (*b*) contraction of the perfusion bed.

Nonhomogeneous lung function. Since both the ventilation and volume equations (17 and 27) assume a single compartment lung, it might be argued that $\dot{V}_A/\dot{Q}$ variations will lead to underestimates in both $\dot{V}_{AXe}$ and FRC_{Xe}. The simulated two-compartment lung model shows that this is not necessarily true

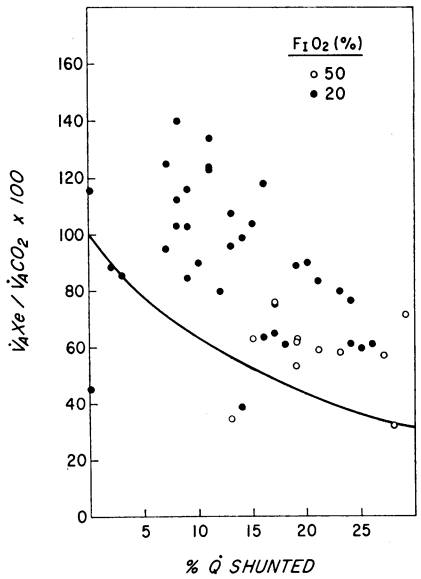

FIGURE 6 Anatomic shunting will cause the ventilation ratio $\dot{V}_{AXe}/\dot{V}_{ACO_2}$ to decrease. This is shown by the simulated two compartment lung model (see Fig. 4). In this case $\dot{V}_{A_1} = 0$ while $\dot{Q}_1$ was increased from 0 to 30% of total flow (solid line). The data from Table II are also plotted using $\dot{Q}_S/\dot{Q} \times 100$ as the abcissa. The closed circles represent the physiologic shunt calculated during room air breathing while the closed circles represent $\dot{Q}_S/\dot{Q}$ at 50% inspired oxygen. Most data points fall to the right of the theoretical curve which represents anatomic shunting. This is probably a reflection of the fact that $\dot{Q}_S/\dot{Q}$, the physiologic shunt is very sensitive not only to anatomic shunts but also to other $\dot{V}_A/\dot{Q}$ imbalances. The ventilation ratio $\dot{V}_{AXe}/\dot{V}_{ACO_2}$ is probably less sensitive to these other $\dot{V}_A/\dot{Q}$ imbalances.

(Fig. 7). In the presence of large intrapulmonary shunts, FRC_{Xe} may increase or decrease depending upon the distribution of air volume. On the other hand, it may be shown that if ventilation and perfusion are uniform, air volume inhomogeneities will not lead to errors in FRC_{Xe}.

In the case of acute bronchial obstruction, right-to-left shunts may occur through nonventilated but air-containing lung. This leads to an overestimate in FRC_{Xe} but an underestimate in FRC_{He} since the air distal to the obstructed airway will not equilibrate with helium. The volume ratio FRC_{Xe}/FRC_{He} will increase even though the ventilation ratio has been shown to decrease (Fig. 6). The data in the seriously ill patients show that $\dot{V}A_{Xe}/\dot{V}A_{CO_2} = 0.539$ while $FRC_{Xe}/FRC_{He} = 0.737$. This is consistent with intrapulmonary shunting occurring, at least in part, through regions with entrapped air. In the case of perfused atelectatic or airless lung segments, both FRC_{Xe} and $\dot{V}A_{Xe}$ will decrease. $\dot{V}A_{CO_2}$ and FRC_{He} will continue to approximate true ventilation and volume. Therefore, both the ventilation and volume ratios will fall. The use of more soluble gas tracers will reduce these ventilation and volume errors.

A third common example of combined ventilation and volume inhomogeneity is under perfusion or complete failure to perfuse portions of the lung. This will lead to identical underestimates in both $\dot{V}A_{Xe}$ and FRC_{Xe}.[9] When regional flow ceases, neither ventilation nor volume will be measured. FRC_{He} is unaffected. Therefore, while the ventilation ratio remains constant, the volume ratio falls.

These three common examples of ventilation-perfusion inhomogeneity, bronchial obstruction, atelectasis, and physiologic dead space, lead to different effects on the $\dot{V}A_{Xe}/\dot{V}A_{CO_2}$ and FRC_{Xe}/FRC_{He} ratios. Since these pathologic events often occur together, and in varying degree, it is not surprising that there is no significant correlation between the volume ratio and either $\dot{Q}s/\dot{Q}$ or the ventilation ratio (Table II).

Comparison of air volumes measured during breathing and breath-holding demonstrate that FRC_{Xe} was consistently lower than VA_{Xe}, averaging 87.6% (Table III). During breath-holding, VA_{Xe} should be virtually insensitive to inhomogeneities in the distribution of volume and of course ventilation. This is true, particularly as xenon recovery approaches unity. Under these circumstances, the volume measured is simply the sum of the regional volumes (equation 4). In theory therefore, the ratio FRC_{Xe}/VA_{Xe} should reflect the nonhomogeneous $\dot{V}A/\dot{Q}$ distributions present during the breathing phase of these experiments ($\dot{Q}s/\dot{Q} = 0.25$). Experimental data in Fig. 5 (Table II) show that a 25% shunt measured during room air breathing corresponds to a $\dot{V}A_{Xe}/\dot{V}A_{CO_2}$ ratio of 0.6 to 0.7. The FRC_{Xe}/VA_{Xe} fell only to 0.876. These considerations indicate that the right to left shunts, which were ob-

[9] The error in FRC_{Xe} is the same as $\dot{V}A_{Xe}$ illustrated in Fig. 5

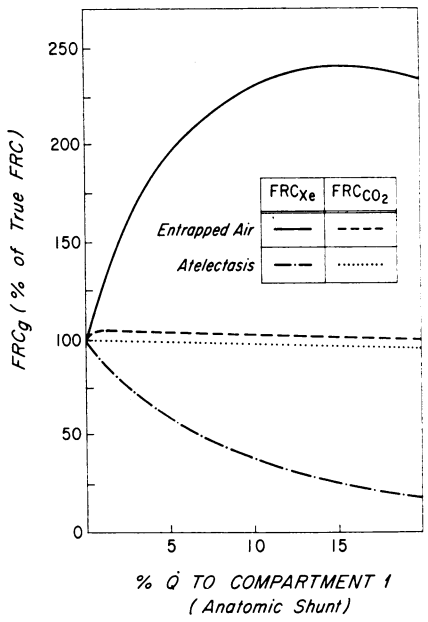

FIGURE 7 Combined inhomogeneities in the distribution of $\dot{V}A/\dot{Q}$ and air volumes lead to errors in FRC_g. The simulated two-comparement lung was used to demonstrate the effects of right-to-left shunts. Total $\dot{V}A$, $\dot{Q}$, and FRC were maintained constant. Ventilation to compartment one $\dot{V}A_1$, was zero while $\dot{Q}_1$, was increased from 0 to 20% of total flow. The air volume in compartment one FRC_1, was either kept constant at zero (atelectasis), or was varied with $\dot{Q}_1$ such that $FRC_1/FRC = Q_1/\dot{Q}$ (entrapped air). The latter case exemplifies air ways obstruction, where there is perfusion of non-ventilated but air-containing lung regions. Δi_{g-r} was calculated from a modification of equation 19:

$$\Delta i_{g-r} = \frac{FRC_1}{\lambda\dot{Q}_1 + \dot{V}A_1}\left(\frac{R_1}{R_1 + R_2}\right) + \frac{FRC_2}{\lambda\dot{Q}_2 + \dot{V}A_2}\left(\frac{R_2}{R_1 + R_2}\right),$$

where the difference in gas and reference tracer transit times in each compartment was weighted by tracer recovery from that compartment. FRC_g was then derived from a modification of equation 27:

$$FRC_g = \frac{\lambda\dot{Q}\Delta i_{g-r}}{R_g}.$$

Elimination of the terms $\dot{Z}$, $\lambda_{gt}V_t$, and $T\dot{V}A/2$ from these equations leads to small errors. The curves show that right-to-left shunts occurring through air containing lung, result in overestimates of FRC_g. The same shunts through regions of atelectasis result in underestimates in FRC_g. The errors are minimized if a very soluble gas is used. The changes in FRC_{CO_2} are illustrated. These curves are entirely theoretical since i_{CO_2} cannot be measured without using labeled CO_2.

served in the experiments of Table III, occurred through lung regions containing entrapped air.

Diffusion. In addition to nonhomogeneities in lung function, diffusion may be a factor in the underestimation of FRC_{Xe}. In theory, volumes measured by indicator techniques are those into which tracer has penetrated before returning to exit the lung via effluent blood. Since the air spaces are large, and many of them are distant from the perfusion bed, the short time available for diffusion interchange during breathing will limit the volumes measured. During breath-holding, there is sufficient time for xenon to evolve into airways distant to alveolae. In one second, xenon diffuses approximately 1.4 cm in air.[10] Therefore over the 1–3 min period required for washout of xenon from the breath-holding lung, it is probable that diffusion interchange occurs with the entire FRC. These differences in the volume accessible to xenon during breathing and breath-holding may in part account for the finding $FRC_{Xe} < V_{AXe}$. Membrane diffusion limitations will accentuate the underestimate in FRC_{Xe}. The relative importance of this membrane phenomenon in sick patients is uncertain.

During breathing, there is no direct data to resolve the question as to how much airway volume is contained within the control volume. In theory, during one normal respiratory cycle there are no oxygen concentration gradients from respiratory bronchiles to alveoli (14). Therefore, the minimum volume included in FRC_{Xe} encompasses those distal conducting airways, contiguous and in concentration equilibrium with perfused alveoli. If the entire lung is perfused and $\dot{V}_A/\dot{Q}$ ratios are uniform, FRC_{Xe} should approach V_{AXe} and FRC_{He}. Any difference in FRC_{Xe} and FRC_{He} under these circumstances will be due to anatomic dead space.

Perfusion bed. Regional inhomogeneities in blood flow result in underestimates in both $\dot{V}_{AXe}$ and FRC_{Xe} (Fig. 5). The effect is most pronounced when flow is completely interrupted. All ventilation to, and volume contained in this region of physiologic dead space will be excluded from tracer measurement.

Application of indicator methology. Tracer measurements of extravascular tissue volumes, alveolar ventilation, and air volumes must be interpreted in light of the distribution of blood flow, ventilation, and air volumes. Failure to perfuse lung segments will result in underestimates of V_t, $\dot{V}_A$, and FRC. Nonuniform distribution of ventilation will lead to underestimates in $\dot{V}_A$, and either under or overestimates in FRC depending upon the distribution of volume. These errors are significant, particularly in sick patients, and limit the independent use of indicator methods.

[10] Based on the relationship $(\bar{X}^2)^{\frac{1}{2}} = \sqrt{2Dt}$, where $(\bar{X}^2)^{\frac{1}{2}}$ is the root mean square diffusional displacement. D is the diffusion coefficient and t is time in seconds (6).

Combination of tracer techniques with other measurements may circumvent these problems. Thus, if it can be shown that the $\dot{V}_{AXe}/\dot{V}_{ACO_2}$ ratio is unity, FRC_{Xe} will be a precise estimate of the volume of air surrounding the perfusion bed. This bed can also be described by the ratio FRC_{Xe}/V_t (Table II). In addition, FRC_{Xe}/FRC_{He} will provide an estimate of the size of the perfusion bed, and when divided into V_t will yield total tissue volume.

The errors inherent in these indicator methods can be used to advantage to provide information concerning nonhomogeneity. The simultaneous use of gases of different solubilities may permit understanding of the type and degree of maldistributions of volume and ventilation which occur in pulmonary disease (15–17). Interpretation of such data can offer insights into pathophysiologic mechanisms. The ability to distinguish flow through nonventilated but air-containing regions, from flow through regions of alveolar collapse may serve to identify airway obstructions or alveolar instability as a cause of right-to-left shunting.

ACKNOWLEDGMENTS

The authors thank Dr. Edward A. Gaensler for his constructive comments and criticism of the manuscript and Dr. Herbert Teager for his assistance in writing the computer program for analysis of the indicator curves. The research was supported by the U. S. Army Medical Research and Development Command, Contract no. DADA-17-67-C-7149 and National Institutes of Health Grant no. GMP-5-PO1-17366-02.

REFERENCES

1. West, J. B. 1971. Causes of carbon dioxide retention in lung disease. *N. Engl. J. Med.* **248**: 1232.
2. Prys Roberts, C., J. F. Nunn, R. H. Dobson, E. H. Robinson, R. Greenbaum, and S. H. Harris. 1967. Radiologically undetectable pulmonary collapse in the supine position. *Lancet.* **2**: 399.
3. Monaco, V., R. Burdge, J. Newell, R. P. Leather, and S. R. Powers, Jr. 1971. Clinical significance of the functional residual capacity in the post-injury state. *Surg. Forum* **22**: 42.
4. Pontoppidan, H., B. Geffin, and E. Lowenstein. 1972. Acute respiratory failure in the adult. *N. Engl. J. Med.* **287**: 690.
5. Zierler, K. L. 1962. Circulation times and the theory of indicator-dilution methods for determining blood flow and volume. *Handb. Physiol.* **1**: 585.
6. Chinard, F. P., R. Effros, W. Pearl, and M. Silverman. 1967. Organ vascular and extravascular compartments in vivo. *AEC Symp. Ser., Compartments Pools Spaces.* **11**: 381.
7. Chinard, F. P., T. Enns, and M. F. Nolan. 1961. Diffusion and solubility factors in pulmonary inert gas exchanges. *J. Appl. Physiol.* **16**: 831.
8. Goresky, C. A., R. F. P. Cronin, and B. E. Wangel. 1969. Indicator dilution measurements of extravascular water in the lungs. *J. Clin. Invest.* **48**: 487.
9. Yeh, S.-Y., and R. E. Peterson. 1965. Solubility of krypton and xenon in blood, protein solutions, and tissue homogenates. *J. Appl. Physiol.* **20**: 1041.

10. Rochester, D. F., R. A. Brown, Jr., W. A. Wichern, Jr., and H. W. Fritts, Jr. 1967. Comparison of alveolar and arterial concentrations of ^{85}Kr and ^{133}Xe infused intravenously in man. *J. Appl. Physiol.* **22**: 423.
11. Herman, A. H., R. E. Justice, and H. B. Hechtman. 1970. An improved system for study of the in vitro perfused lung. The Proceedings of the 23rd Annual Conference on Engineering in Medicine and Biology, Washington, D. C. **12**: 253.
12. Hechtman, H. B., R. E. Justice, and A. H. Herman. 1970. A mercury injection system for rapid anaerobic collection of small blood samples. *J. Appl. Physiol.* **29**: 528.
13. Anderson, A. M., and J. Ladefoged. 1965. Relationship between hematocrit and solubility of ^{133}Xe in blood. *J. Pharm. Sci.* **54**: 1684.
14. LaForce, R. C., and B. M. Lewis. 1970. Diffusional transport in the human lung. *J. Appl. Physiol.* **28**: 291.
15. West, J. B. 1969. Effect of slope and shape of dissociation curve on pulmonary gas exchange. *Resp. Physiol.* **8**: 66.
16. Hechtman, H. B., M. H. Reid, B. C. Dorn, R. E. Justice, and R. D. Weisel. 1972. Shunting in the lung: a two-compartment model. *Surgery.* **72**: 443.
17. Farhi, L. E. 1967. Elimination of inert gases by the lung. *Resp. Physiol.* **3**: 1.
18. Chinard, F. P., and T. Enns. 1954. Transcapillary pulmonary exchange of water in the dog. *Am. J. Physiol.* **178**: 197.
19 Levine, O. R., R. B. Mellins, and A. P. Fishman. 1965. Quantitative assessment of pulmonary edema. *Circ. Res.* **17**: 414.
20. Ramsey, L. H., W. Puckett, A. Jose, and W. W. Lacy. 1964. Pericapillary gas and water distribution volumes of the lung calculated from multiple indicator dilution curves. *Circ. Res.* **15**: 275.
21. Hechtman, H. B., and A. H. Herman. Indicator dilution studies of lung functions. *Symposia. 6th Eur. Conf. Microcirculation.* Karger, Basel, Switzerland. 18.
22. Cander, L., and R. E. Forster. 1959. Determination of pulmonary parenchymal tissue volume and pulmonary capillary blood flow in man. *J. Appl. Physiol.* **14**: 541.
23. Cook, C. D., J. Mead, G. L. Schreiner, N. R. Franks, and J. M. Craig. 1959. Pulmonary mechanics during induced pulmonary edema in anesthetized dogs. *J. Appl. Physiol.* **14**: 177.
24. Mead, J., and C. Collier. 1959. Relation of volume history of lungs to respiratory mechanics in anesthetized dogs. *J. Appl. Physiol.* **14**: 669.